УДК 544.228 54.057

**T. SALAMAKHA, Y. TRATSIAK,
G. SHEVCHENKO, V. ZHURAVKOV**

THE ENHANCE OF THE LUMINESCENT PROPERTIES OF BaI_2 : Eu FINE POWDERS BY Au NANOPARTICLES

*Research Institute for Physical Chemical Problems
of the Belarusian State University, Minsk, Belarus*

Приведены результаты синтеза BaI_2 : Eu, содопированного наночастицами Au (НЧ Au), с использованием двухстадийного метода. Установлено влияние содопирования НЧ Au на структурные, морфологические и люминесцентные свойства образцов BaI_2 : Eu. По данным рентгеноструктурного анализа образцы BaI_2 : Eu в основном состоят из фаз BaI_2 и $BaI_2 \cdot H_2O$. С увеличением количества НЧ Au в образцах обнаружено уменьшение параметров ячейки фазы BaI_2. Спектры люминесценции (СЛ) состоят из уширенных интенсивных полос люминесценции с максимумами при 420 нм, которые связаны с $5d$–$4f$ переходом ионов Eu^{2+}, и малоинтенсивных полос с максимумами при 615 нм, которые относятся к люминесценции Eu^{3+}. Интенсивность полосы люминесценции ионов Eu^{2+} максимальна для образца с 0,05 масс. % НЧ Au. Согласно результатам исследования люминесценции, проводимого в течение 30 дней, содопирование образцов BaI_2 : Eu НЧ Au приводит к увеличению значений интенсивности люминесценции в 2,2 раза. Показана возможность быстрой идентификации состава образцов BaI_2 : Eu путем анализа спектров люминесценции.

The synthesis of BaI_2 : Eu co-doped with Au nanoparticles (AuNPs) using the two-stages approach is reported. The influence of the AuNPs co-doping on the structural, morphological and luminescent properties of BaI_2 : Eu samples is established. According to X-ray diffraction analysis BaI_2 : Eu samples mainly consist of BaI_2 and $BaI_2 \cdot H_2O$ phases. A slight decrease of the cell unit parameters for BaI_2 phase with an increase in AuNPs quantity is found. The photoluminescence (PL) spectra are presented by broad and strong emission bands peaking at 420 nm which are related to the Eu^{2+} $5d$–$4f$ transition and low-intensive bands peaking at 615 nm which are attributed to the PL of Eu^{3+}. Intensity of Eu^{2+} PL band reaches maximum for the sample with 0.05 wt. % AuNPs. The results of the PL study carried out for 30 days demonstrate significant improvement of the PL intensity values for BaI_2 : Eu samples up to about a factor 2.2 by the co-doping with AuNPs. The possibility of rapid composition identification for BaI_2 : Eu samples using the PL analysis is shown.

Ключевые слова: люминесценция; Eu^{2+}; иодид бария; тонкодисперсные порошки; Au; наночастицы.

Keywords: luminescence; Eu^{2+}; barium iodide; fine powders; Au; nanoparticles.

The relevance of luminescent materials is explained by their application in different fields of human's activity and life, including high energy physics, photonics, medicine, lighting, security, agriculture and others [1–3]. Nowadays the search for new and the improvement of existing cheap and effective luminescent materials is an actual task of practical interest due to the absence of an ideal phosphor that can be used across the board [4]. One of the cost effective and promising luminescent materials is halide based compounds, doped with rare earths, mostly with Eu ions. Such compounds are very perspective for application in various fields from high energy physics (SrI_2 : Eu) to solar energy (halide based perovskites) [5, 6]. Among halide based compounds alkali-earth halides doped with Eu ions are attractive for research due to their potential for luminescent applications. For instance, all these materials can be used as components for light emitting diodes (LEDs) and europium-doped barium mixed halides are widely used as phosphors in X-ray image intensifying screens and in imaging plates for medical imaging [7, 8].

The choice of europium as the doping ion is explained by its specific characteristics among other rare-earth dopants. Europium can exist in two stable charging states: Eu^{2+} and Eu^{3+} which under UV excitation both emit in visible spectral region predominantly in blue and red areas, respectively [9, 10]. Yet, in several studies Eu^{3+} emission in blue and green region was also discovered [11, 12]. In recent works Eu^{2+} and Eu^{3+} simultaneous existence in phosphors was proved allowing to shift resulting color of material's luminescence from blue to red [13]. While *f–f* emission of Eu^{3+} ions leads to narrow emission bands [14], Eu^{2+} ions demonstrate broad *d–f* emission band which maximum position depends on a crystalline surrounding of the luminescent center [15, 16]. Thus, luminescent characteristics of phosphors doped with europium ions can be controlled by a change of Eu^{2+}/Eu^{3+} ratio and variation of Eu^{2+} local environment.

From the literature it is known that co-doping of luminescent materials with various ions and nanoparticles significantly affects their optical, electrical and magnetic properties [17–20]. It has been shown that co-doping of BaBrCl : Eu single crystals with Au ions had improved their photoluminescence intensity, scintillation light output and reduced long time after glow; and co-doping of Eu complex and Eu doped germanate films with Au nanoparticles (AuNPs) had enhanced their luminescence intensities [21–23]. Moreover the feature of nanoparticles is a possibility to absorb radiation in various areas of spectrum depending on their size and surface morphology which provides variation of structural and luminescent properties inherent to phosphors [24, 25].

In accordance with the foregoing, the aim of this work was to establish the effect of AuNPs co-doping on the structural, morphological and luminescent properties of BaI_2 : Eu.

EXPERIMENTAL SECTION

Synthesis. $Ba(NO_3)_2$, $Eu(NO_3)_3 \cdot 6H_2O$, NH_4HCO_3, NH_4I, $HAuCl_4$, NaOH and Na_2EDTA were used as starting materials. All reagents were of analytical grade. BaI_2 was prepared by 2 stages approach described earlier: the first stage involved the

synthesis of $BaCO_3$: Eu (precursor) converted into BaI_2 : Eu in the second stage [26, 27]. AuNPs in the form of Au sol in the amount of 0, 0.01, 0.05, 0.1 and 0.2 wt. % were added to the precursor on the first stage of synthesis.

For Au sol preparation and solutions containing 0.023 mole/dm^3 $HAuCl_4$, 0.075 mole/dm^3 NaOH and 0.008 mole/dm^3 Na_2EDTA were used. NaOH solution was added to Na_2EDTA solution to the required pH level (10.5) under continuous stirring. The obtained solution was heated (~ 2 °C/min) up to 90 °C, then $HAuCl_4$ solution was added. The mixture was held at this temperature for 30 min. Au concentration in this sol was $5 \cdot 10^{-4}$ mole/dm^3. Synthesized Au sol was of dark-cherry color [28].

$BaCO_3$: Eu powder was obtained by reverse precipitation. At first the required quantity of the solution containing 0.1 mole/dm^3 of $Eu(NO_3)_3$ was added into 0.2 molar $Ba(NO_3)_2$ solution. $Eu(NO_3)_3$ was added in the amount corresponding to the replacing of 2 at. % of Ba^{2+} ions with Eu^{3+} ions. The mixture of nitrates was then added dropwise into 1.2 molar solution of NH_4HCO_3 under continuous stirring. The resulting $BaCO_3$: Eu precipitate was isolated by centrifugation and washed 2 times with distilled water. The required quantities of Au sol were added to $BaCO_3$: Eu suspensions and exposed to the continuous stirring for 1 h. Then the resulting mixtures were dried in air at 80 °C for 12 h. Since further conversion of $BaCO_3$ to BaI_2 was occurring, the amounts of AuNPs additive were calculated on the basis of Ba weight in samples. Taking into account that AuNPs concentration in sol was known accurately, the quantity of sol was recalculated in milliliter and added to precursor suspension with a known quantity of $BaCO_3$: Eu. After stirring for 10–15 min the suspension became separated itself and transparent solution under precipitate was observed. Thus, one can conclude that AuNPs were combined with $BaCO_3$ particles.

$BaCO_3$: Eu co-doped with AuNPs and NH_4I powders were mixed in the agate mortar and then transferred into a quartz boat which was placed into a quartz tube with subsequent argon (Ar) flux for 10 min. The tube was moved into the furnace preheated up to 400 °C and annealed for 30 min under constant Ar flow. After that samples were spontaneously cooled to the room temperature (~ 50 °C/min) in a quartz tube under the Ar flow. The obtained light-gray iodide powders were transferred into containers that were tightly sealed. Depending on the amount of AuNPs used in the synthesis samples have been designated as 0 (0 wt. %), 1 (0.01 wt. %), 2 (0.05 wt. %), 3 (0.1 wt. %), 4 (0.2 wt. %).

The whole process on the second stage of the synthesis can be described by the following equation:

$$BaCO_3 : Eu + 4NH_4I \rightarrow BaI_2 : Eu + CO_2 + I_2 + H_2 + 4NH_3 + H_2O. \quad (1)$$

It should be mentioned that the influence of the precursor morphology and Eu ions concentration on the structural, morphological and luminescent properties of the BaI_2 : Eu powders have been studied previously [26, 29].

Characterization. X-ray diffraction patterns of the synthesized samples were collected by PANalytical Empyrean X-ray diffractometer with CuK_α radiation source

(λ = 1.5406 Å) in the 2θ range of 23–75°. To prevent the contact of iodide samples with water from atmosphere they were placed in a holder between two polyethylene films. The X-ray diffraction patterns of these films showed a reflection at 23.8° 2θ. The size of the coherent scattering region (CSR) and microstress values were determined from the full width at a half maxima (FWHM) of X-ray diffraction (XRD) lines approximated by the Voight functions using Williamson–Hall method [30]. Standard corrections for the CuK_α radiation were taken into account. The processing of data was made in Fityk, WinPLOTR-2006 and DICVOL06 programs of FullPROF.

Morphology of the samples was studied by scanning electron microscope (SEM) LEO-1420 with a 20 000 magnification.

Room temperature photoluminescence measurements were provided by Jobin Yvon Fluoromax 2 spectrofluorimeter. The photoluminescence (PL) and photoluminescence excitation (PLE) spectra were collected from ~1 mm-thick layers of samples placed onto a quartz plate. All the PL and PLE spectra were measured at 298 K. For performing the PL measurements depending on time each sample was placed between two tightly sealed pieces of quartz glass and between measurements was stored in a hermetic container filled with Ar to avoid the interaction with atmosphere.

RESULTS AND DISCUSSION

The synthesized Au sol of dark-cherry color has plasmon band in the absorption spectrum at λ_{max} ~ 525 nm (Fig. 1, *a*). The absorption spectrum shape and plasmon position are typical for AuNPs of spherical shape [31].

TEM image of Au sol is shown in Fig. 1, *b*. At the used pH value of 10.5 Au sol consists of nanoparticles with uniform shape and size. The average diameter of the AuNPs in sol is 15.1 ± 2.2 nm.

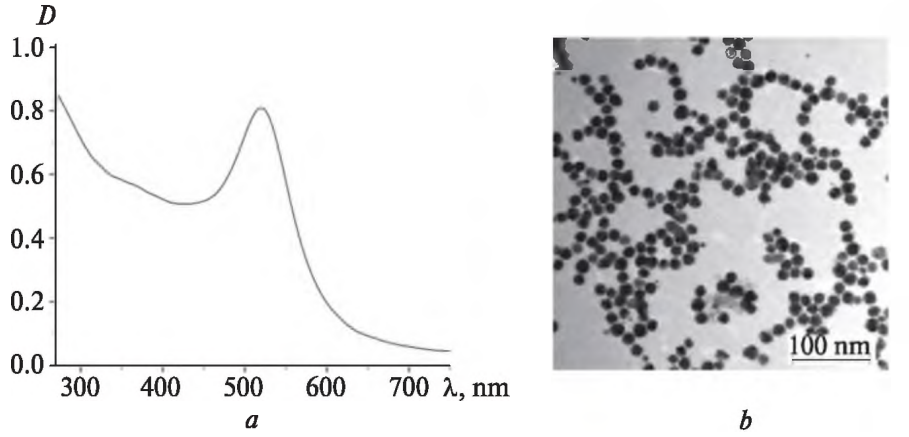

a *b*

Fig. 1. Normalized optical absorption spectrum of the AuNPs (*a*);
TEM image of the AuNPs (*b*)

The XRD patterns of the samples 0–4 are shown in Fig. 2. They exhibit reflections attributable to 2 phases: BaI_2 (Powder Diffraction File № 73–1849) and $BaI_2 \cdot H_2O$ (PDF № 39–1300). For samples 0, 1, 2 and $3BaI_2$ phase is prevailing, while for sample 4 $BaI_2 \cdot H_2O$ phase is dominating. The presence of reflections for $BaI_2 \cdot H_2O$ phase in different amounts for each sample on the XRD patterns can be a result of interaction of the samples with water vapor released in the synthesis process (Eq. 1) or during samples moving into containers.

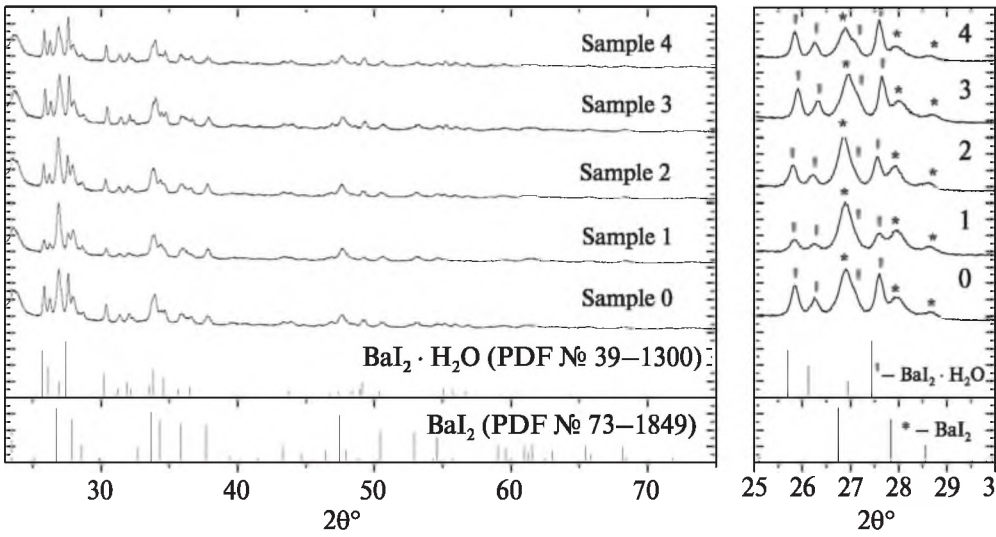

Fig. 2. XRD patterns of the samples 0–4. Broadened reflection with maximum at 23.8° originates from a polyethylene films. The numbers correspond to data in Table 1

Calculated values of the unit cell parameters, CSR size, and microstress (ε) for the BaI_2 phase in the samples 0–4 are listed in Table 1. The obtained values of the unit cell parameters are in agreement with the tabulated data for the BaI_2 phase (PDF № 73–1849).

Table 1

Unit cell parameters, CSR sizes, and microstress values for the synthesized samples 0–4

Sample	Compound	*a*, Å	*b*, Å	*c*, Å	Cell Volume	CSR, nm	ε, 10^{-5}
0	BaI_2	10.6930(51)	8.8985(38)	5.2993(25)	504.24	42.3	11.2
1	BaI_2	10.6110(83)	8.8420 (76)	5.2447 (83)	492.07	45.5	13.4
2	BaI_2	10.6185(88)	8.8522(80)	5.2337 (87)	491.95	43.3	6.6
3	BaI_2	10.6226(57)	8.8341(69)	5.2727(26)	494.79	46.9	6.3
4	BaI_2	10.6030(25)	8.8286(33)	5.2643(13)	492.79	68.7	8.7

As can be seen from Table 1 the co-doping of BaI_2 : Eu samples with AuNPs leads to a slight decrease of the unit cell parameters and, as a result, of the cell volumes. Decrease in the cell volumes is most probably related with a partial substitution of Ba^{2+} onto Au ions. AuNPs can react with the iodine released during the synthesis leading to the formation of such compounds as AuI, AuI_2^-, AuI_4^- [32–34]. Since the values of ionic radii for Au^+ (AuI and AuI_2^- compounds) and Ba^{2+} are close (1.37 and 1.47 Å, respectively, see Table 2), one can assume the possibility of substitution of larger Ba^{2+} ions onto smaller Au^+ ions in the BaI_2 structure. Taking into account that ion radius for Au^{3+} ions (AuI_4^- compound) is 2.2 times smaller than that for Ba^{2+} the possibility of the incorporation of Au^{3+} ions into the BaI_2 structure should be considered. The formation of AuI_4^- occurs in a very small amount, due to almost complete displacement of $AuI_2^- + I_2 \leftrightarrow AuI_4^-$ reaction to the left. Nevertheless, AuI_4^- availability in crystalline lattice as a pair for Au^+ for charge compensation can not be excluded [34]. Localization of Au^{3+} on the Ba^{2+} positions should also lead to decrease of the cell volumes.

Table 2

Ionic radii for Ba^{2+}, Au^+ and Au^{3+} ions (coordination numbers are 9, 4 and 6, respectively) [35]

Ion	Ba^{2+}	Au^+	Au^{3+}
Ion radius, Å	1.47	1.37	0.68

The difference in the CSR values for the samples 0–4 (Table 1) can be connected with the influence of AuNPs on the mass transfer process occurring during the synthesis. As one can assume AuNPs should be localized mostly on the surface of the precursor particles. It is possible that such localization decreases the intensity of mass transfer between the precursor aggregates during the barium iodide formation on the second stage of the synthesis. As a result, the growth of barium iodide particles within the aggregates becomes more intensive. With an increase in Au content in samples the microstress values are decreasing. This fact can be connected with the enlargement of crystallites size and perfection of their structure due to the decrease in the ratio between particles surface and their volume. As a result, relative quantity of the surface defects as compared with those in the particles volume is diminished.

SEM images of the $BaCO_3$: Eu and BaI_2 : Eu samples are presented in Fig. 3. They illustrate the effect of Au content on their microstructure. $BaCO_3$: Eu precursor samples consist of aggregates composed by particles 0.7–3.0 μm in size. BaI_2 : Eu samples are similar in their morphology to precursors: they also consist of spheroidal aggregates that are smaller in size (0.7–2.0 μm).

The difference in aggregates size of BaI_2 : Eu and $BaCO_3$: Eu samples is explained by various crystalline structures, densities, and, as a result, volumes of BaI_2 and $BaCO_3$ particles with the same quantity of Ba^{2+} ions. Despite the observed difference in the CSR values for the samples 0–4, it should be noted that co-doping of samples with

AuNPs up to 0.2 wt. % does not significantly influence $BaCO_3$ and BaI_2 particles morphology. In this work the formation of $BaCO_3$ particles aggregates follows a colloid aggregation mechanism, which means that each aggregate consists of small crystallites. Although the Au content affects the CSR size of crystallites, it doesn't influence the resulting aggregates morphology.

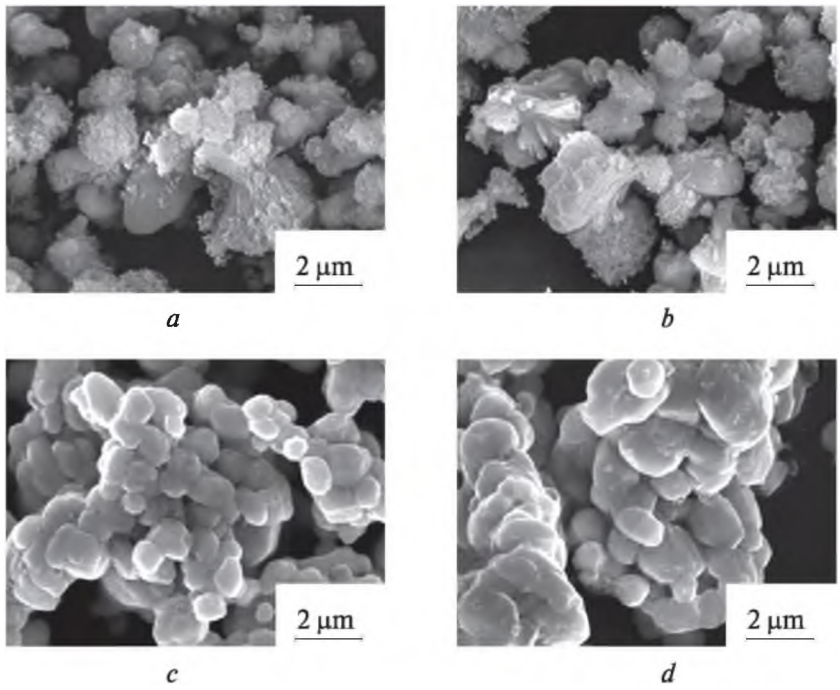

Fig. 3. SEM images of the $BaCO_3$: Eu (*a*, *b*) and the BaI_2 : Eu (*c*, *d*) samples with 0 wt. % (*a*, *c*) and 0.2 wt. % (*b*, *d*) of AuNPs

The PL and PLE spectra of the samples 0–4 are presented in Fig. 4. The broad PLE bands (Fig. 4, *a*) within the 255–395 nm was referred to the Eu^{2+} $4f \rightarrow 5d$ transition [36]. The PL bands are narrow and close to symmetrical with maxima at 420 nm (Fig. 4, *b*). Thus, these bands correspond to the inter-configurational $4f^6 5d^1 \rightarrow 4f^7$ radiation transition of Eu^{2+} in BaI_2 structure [37]. The PL spectra also have low-intensive bands characteristic for Eu^{3+} with maxima at 615 nm [38], which indicates the incomplete $Eu^{3+} \rightarrow Eu^{2+}$ transition during the synthesis or the surface oxidation of Eu^{2+} to Eu^{3+}. A significant concentration effect of the AuNPs co-doping on the luminescence properties of samples is clearly observed. As one can see from Fig. 4, maximum PL intensity from the signal is observed for the sample 2.

In the literature it is pointed out that when the amount of oxygen vacancies is small they might act as the sensitizers for the energy transfer to the rare earth ion due to the strong mixing of charge transfer states. It results in the highly enhanced

luminescence. When oxygen vacancies are in the excess they inevitably destroy the host crystallinity, which leads to quenching of the luminescence [39–41].

A significant part of the oxygen contamination in barium halide systems comes from surface hydrate reactions due to the materials hygroscopicity. Oxygen ions can enter such systems doped with europium and act as oxygen-vacancy centers. In europium-doped BaFCl, for instance, oxygen vacancies are actually hole traps, because the divalent oxygen ion (O_2^-) occupying the halogen site (Cl^- or F^-) prefers to capture a hole to balance its charge [42].

In accordance with the foregoing we suppose that the increase in PL intensity can be explained by two possibilities. The first one is due to the AuNPs leading to a lower probability of charge carrier trapping by the traps mentioned above [21]. The second possibility is due to more effective charge transfer to the luminescent ion by AuNPs with the formation of Eu^{2+}–Au_x^+ centers. Possible presence of AuI, AuI_2^-, AuI_4^- has to be taken into account. This possibility is mentioned in the study of Malashkevich G. E. et al. [23]. Nevertheless, we have to admit that the raised question requires more thorough study.

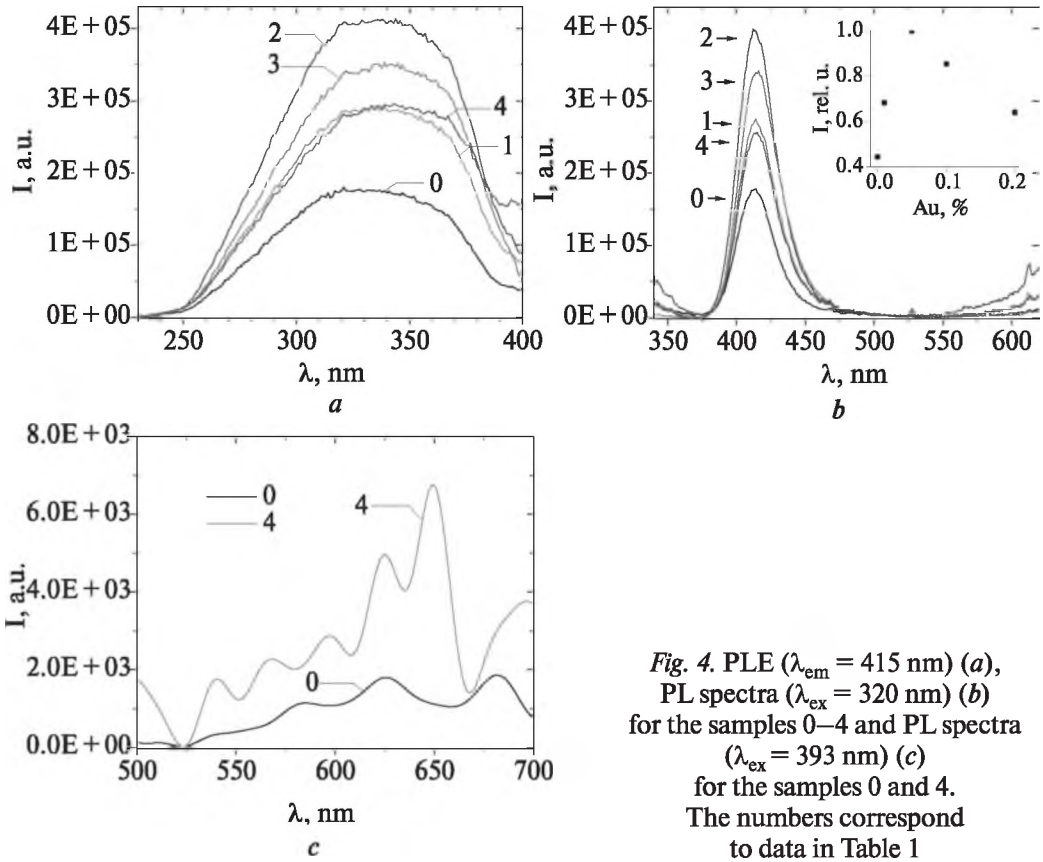

Fig. 4. PLE (λ_{em} = 415 nm) (*a*), PL spectra (λ_{ex} = 320 nm) (*b*) for the samples 0–4 and PL spectra (λ_{ex} = 393 nm) (*c*) for the samples 0 and 4. The numbers correspond to data in Table 1

As one can see from Fig. 5, *a*, the co-doping with AuNPs improves significantly the luminescence intensity values (up to about a factor 2.2) for BaI_2 : Eu samples with maintaining this difference at least for 30 days. It can be explained by 3 hypotheses: 1) capturing of electrons that are created in the process of AuI, AuI_2^- and AuI_4^- formation by Eu^{3+} ions with the formation of Eu^{2+} ions [43]; 2) the field enhancement effect caused by the surface plasmon of the AuNPs [22, 44]; 3) the impact of AuNPs on the suppression of trapping centers in BaI_2 : Eu.

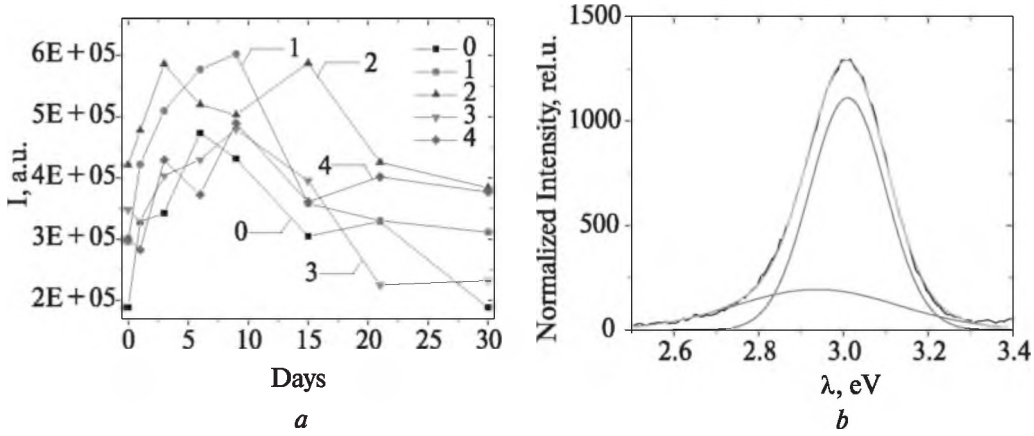

a *b*

Fig. 5. Dependence of the PL intensity (λ_{ex} = 320 nm) for the samples 0–4 on time (*a*); PL spectrum for the sample 0 fitted with 2 Gaussian functions (*b*). The numbers correspond to data in Table 1

It is known that the position of Eu^{2+} luminescence band depends on its crystalline surrounding [45]. Considering that BaI_2 is hygroscopic material and can exist in different hydrate forms, e. g. $BaI_2 \cdot H_2O$, $BaI_2 \cdot 2H_2O$ and $BaI_2 \cdot 6H_2O$, it is important to have a possibility of quick composition analysis of such samples for better understanding the Eu^{2+} luminescence origin. The opportunity of using the PL spectra splitting for the rapid composition identification, taking into account higher sensitivity of PL analysis in comparison with XRD, was estimated. It occurred that PL spectra of the samples 0–4 are the best fitted with 2 Gaussian functions (Fig. 5, *b*). Thus, according to the results given in Table 3 the PL spectra of samples 0–4 are complex and consist of 2 overlapped bands with maxima at 412 nm (3.01 eV) and 422–427 nm (2.94–2.90 eV), which indicates the distribution of Eu^{2+} over 2 crystalline surroundings.

Table 3

Values of the PL bands maxima for the samples 0–4

Sample	0	1	2	3	4
Band maximum, eV	3.01	3.01	3.01	3.01	3.01
Band maximum, nm	412	412	412	412	412
Band maximum, eV	2.94	2.89	2.90	2.90	2.91
Band maximum, nm	422	427	427	427	426

For the sample 0 a band with a maximum at 412 nm can be attributed to BaI_2 phase and, therefore, the minor band with a maximum at 422 nm belongs to $BaI_2 \cdot H_2O$ phase [46]. It is confirmed by the existence of these 2 phases in the XRD patterns. Hence, the PL spectrum splitting can be used for the rapid phases identification of alkali-earth iodide samples.

CONCLUSIONS

In this study the original two-stages approach to the synthesis of iodide samples co-doped with AuNPs has been used. According to XRD data the obtained samples include BaI_2 and $BaI_2 \cdot H_2O$ phases. The presence of $BaI_2 \cdot H_2O$ phase in the XRD patterns has been explained by the absorption of water that was released during the synthesis or from the surrounding atmosphere. The slight decrease of the unit cell parameters for the BaI_2 phase has been found to be connected with the substitution of Ba^{2+} ions onto Au^{+} ions and the incorporation of Au^{3+} ions into the BaI_2 structure. It has been shown that the addition of AuNPs up to 0.2 wt. % does not influence BaI_2 : Eu particles morphology. For all the samples the PL spectra have demonstrated Eu^{2+} emission band in the BaI_2 structure (λ_{em} = 420 nm) and low-intensive band peaking at 615 nm characteristic for the Eu^{3+}. The presence of Eu^{3+} has been explained by the incomplete $Eu^{3+} \rightarrow Eu^{2+}$ transition during the synthesis or surface oxidation of Eu^{2+}. The results of the PL study, that has been carried out for 30 days, have demonstrated that the addition of AuNPs improved significantly PL intensity values by a factor up to 2.2. Three hypotheses explaining this phenomenon have been suggested: 1) the transfer of electrons created in the process of AuI, AuI_2^- and AuI_4^- formation to the BaI_2 : Eu; 2) the field enhancement effect caused by the surface plasmon of the AuNPs; 3) the influence of the AuNPs on the number of trapping centers in BaI_2 : Eu. The application of the PL analysis for the rapid identification of BaI_2 : Eu samples composition has been shown. It has been discovered that the PL spectra of the samples 0–4 are the best fitted with 2 Gaussian functions that proves the distribution of Eu^{2+} over 2 crystalline surroundings which are the BaI_2 and $BaI_2 \cdot H_2O$ phases according to XRD.

REFERENCES

1. *Faoite D. De, Hanlon L., Roberts O.* [et al.]. Development of glass-ceramic scintillators for gamma-ray astronomy // J. Phys. Conf. Ser. 2015. P. 0120021–0120026.

2. *Nikl M., Yoshikawa A.* Recent R&D Trends in Inorganic Single-Crystal Scintillator Materials for Radiation Detection // Adv. Opt. Mater. 2015. Vol. 3. P. 463–481.

3. *Blasse G.* Scintillator Materials // Chem. Mater. 1994. Vol. 6. P. 1465–1475.

4. *Feldmann C., Jüstel T., Ronda C. R., Schmidt P. J.* Inorganic luminescent materials: 100 Years of research and application // Adv. Funct. Mater. 2003. Vol. 13, № 7. P. 511–516.

5. *Yanagida T., Koshimizu M., Okada G.* [et al.]. Comparative study of nondoped and Eu-doped SrI_2 scintillator // Opt. Mater. (Amst). 2016. Vol. 61. P. 119–124.

6. *Bala A., Kumar V.* Stability of the Eu^{2+} Dopant in $CsPbBr_3$ Perovskites: A First-Principles Study // J. Phys. Chem. C. 2019. Vol. 123. P. 6965–6969.

7. *Jestin Lenus A., Sornadurai D., Govinda Rajan K., Purniah B.* Luminescence behaviour of Eu^{2+}-doped BaClI and BaBrI // Mater. Lett. 2002. Vol. 57. P. 635–638.

8. *Terraschke H., WickledерC.* UV, Blue, Green, Yellow, Red, and Small: Newest Developments on Eu^{2+}-Doped Nanophosphors // Chem. Rev. 2015. Vol. 115. P. 11352–11378.

9. *Gahane D. H., Kokode N. S., Muthal P. L.* [et al.]. Luminescence of Eu^{2+} in some iodides // Opt. Mater. (Amst). 2019. Vol. 32. P. 18–21.

10. *Kalpana T., Brik M. G., Sudarsan V.* [et al.]. Influence of Al^{3+} ions on luminescence efficiency of Eu^{3+} ions in barium boro-phosphate glasses // J. Non. Cryst. Solids. 2015. Vol. 419. P. 75–81.

11. *Dejneka M., Snitzer E., Riman R. E.* Blue, green and red fluorescence and energy transfer of Eu^{3+} in fluoride glasses // J. Lumin. 1995. Vol. 65. P. 227–245.

12. *Liu X., Lin C., Lin J.* White light emission from Eu^{3+} in $CaIn_2O_4$ host lattices // Appl. Phys. Lett. 2007. Vol. 90. P. 081904.

13. *Xie H., Lu J., Guan Y.* Chem Inform Abstract: Abnormal Reduction, $Eu^{3+} \rightarrow Eu^{2+}$, and Defect Centers in Eu^{3+}-Doped Pollucite, $CsAlSi_2O_6$, Prepared in an Oxidizing Atmosphere // Inorg. Chem. 2014. Vol. 53. P. 827–834.

14. *Zhai Y., You Z., Liu Y.* Properties of red-emitting phosphors $Sr_2MgSi_2O_7 : Eu^{3+}$ prepared by gel-combustion method assisted by microwave // J. Rare Earths. 2012. Vol. 30. P. 114–117.

15. *Biswas K., Sontakke A. D., Sen R., Annapurna K.* Luminescence properties of dual valence Eu doped nano-crystalline BaF_2 embedded glass-ceramics and observation of Eu^{2+} Eu^{3+} energy transfer // J. Fluoresc. 2012. Vol. 22. P. 745–752.

16. *Tratsiak Y., Buryi M., Babin V.* [et al.]. The effect of binary glass composition on the Eu-ions luminescence properties // Opt. Mater. (Amst). 2019. Vol. 94. P. 356–362.

17. *Pejchal J., Buryi M., Babin V.* [et al.]. Luminescence and scintillation properties of Mg-codoped LuAG : Pr single crystals annealed in air // J. Lumin. 2017. Vol. 181. P. 277–285.

18. *Chen Y., Yang H. K., Park S. W.* [et al.]. Characterization and photoluminescent enhancement of Li^+ corporation effect on $CaWO_4 : Eu^{3+}$ phosphor // J. Alloys Compd. 2012. Vol. 511. P. 123–128.

19. *Liu D., Shi J., Tong L.* [et al.]. $YVO_4 : Eu^{3+}$, $Dy^{3+}@Fe_3O_4$ co-doped nanocomposites: Preparation, luminescent, and magnetic properties // J. Nanoparticle Res. 2012. Vol. 14. P. 1216.

20. *Zhou H., Wu G., Qin N., Bao D.* Dual enhancement of photoluminescence and ferroelectric polarization in Pr^{3+}/La^{3+}-codoped bismuth titanate thin films // J. Am. Ceram. Soc. 2010. Vol. 93. P. 2109–2112.

21. *Shalapska T., Moretti F., Bourret E., Bizarri G.* Effect of Au codoping on the scintillation properties of BaBrCl : Eu single crystals // J. Lumin. 2018. Vol. 202. P. 497–501.

22. *Levchenko V.* Luminescence of Europium complex enhanced by surface plasmons of gold nanoparticles for possible application in luminescent solar concentrators // J. Lumin. 2018. Vol. 193. P. 5–9.

23. *Malashkevich G. E., Chukova O. V., Nedilko S. G.* [et al.]. Influence of Gold Nanoparticles on Luminescence of Eu^{3+} Ions Sensitized by Structural Defects in Germanate Films // J. Phys. Chem. C. 2016. Vol. 120, № 28. P. 15369–15377.

24. *Wackerow S., Seifert G.* Co-doping of glasses with rare earth ions and metallic nanoparticles for frequency up-conversion // Photonics Sol. Energy Syst. III. 2010. P. 77251H.

25. *Hussain T., Zhong L., Danesh M.* [et al.]. Enabling low amounts of YAG : Ce^{3+} to convert blue into white light with plasmonic Au nanoparticles // Nanoscale. 2015. Vol. 7. P. 10350–10356.

26. *Salamakha T., Buryi M., Tratsiak Y.* Effect of Eu-doping on optical, structural and morphological properties of $BaI_2 \cdot nH_2O$ powders // Opt. Mater. (Amst). 2018. Vol. 78. P. 352–359.

27. *Salamakha T. A., Trusova E. E., Tratsiak Y. U.* Preparation and study of the luminescent glass-ceramics based on barium iodide activated with Eu^{2+} // J. Belarusian State Univ. Chem. 2019. Vol. 1. P. 38–44.

28. *Shevchenko G. P., Zhuravkov V. A., Osipovich N. P., Shishko G. V.* Synthesis of gold hydrosols in the presence of Na_2EDTA // J. Belarusian State Univ. Chem. 2019. Vol. 1. P. 86–94.

29. *Tret'yak E. V., Shevchenko G. P., Solomakha T. A., Korzhik M. V.* Effect of precursor morphology on the structural properties, optical absorption, and luminescence of $BaI_2 : Eu^{2+}$, Eu^{3+} // Inorg. Mater. 2017. Vol. 53. P. 307–312.

30. *Williamson G. K., Hall W. H.* X-ray line broadening from filed aluminium and wolfram // Acta Metall. 1953. Vol. 1. P. 22–31.

31. *Moores A., Goettmann F.* The plasmon band in noble metal nanoparticles: An introduction to theory and applications // New J. Chem. 2006. Vol. 30. P. 1121–1132.

32. *Davis A., Tran T., Young D. R.* Solution chemistry of iodide leaching of gold // Hydrometallurgy. 1993. Vol. 32. P. 143–159.

33. *Davis A., Tran T.* Gold dissolution in iodide electrolytes // Hydrometallurgy. 1991. Vol. 26. P. 163–177.

34. *Elding L. I., Skibsted L. H.* Kinetics and Mechanism for Reduction of Ammine and Haloammine Complexes of Gold(III) by Iodide // Inorg. Chem. 1986. Vol. 25. P. 4084–4087.

35. *Shannon R. D.* Revised effective ionic radii and systematic studies of interatomic distances in halides and chalcogenides // Acta Crystallogr. Sect. A. 1976. Vol. 32. P. 751–767.

36. *Wu Y., Boatner L. A., Lindsey A. C.* [et al.]. Defect Engineering in $SrI_2 : Eu^{2+}$ Single Crystal Scintillators // Cryst. Growth Des. 2015. Vol. 15. P. 3929–3938.

37. *Yan Z., Gundiah G., Bizarri G. A.* [et al.]. Eu^{2+}-activated $BaCl_2$, $BaBr_2$ and BaI_2 scintillators revisited // Nucl. Instruments Methods Phys. Res. Sect. A: Accelerators, Spectrometers, Detect. Assoc. Equip. 2014. Vol. 735. P. 83–87.

38. *Almeida R., Silva D. M., Kassab L. R. P., Araújo C. B.* Eu^{3+} luminescence in tellurite glasses with gold nanostructures // Opt. Commun. 2008. Vol. 281, № 1. P. 108–112.

39. *Nagpure I. M., Shinde K. N., Dhoble S. J., Kumar A.* Photoluminescence characterization of Dy^{3+} and Eu^{2+} ion in $M_5(PO_4)_3F$ (M = Ba, Sr, Ca) phosphors // J. Alloys Compd. 2009. Vol. 481. P. 632–638.

40. *Jia D., Yen W M.* Enhanced VK^{3+} center afterglow in $MgAl_2O_4$ by doping with Ce^{3+} // J. Lumin. 2003. Vol. 101. P. 115121.

41. *Sun L., Qian C., Liao C.* [et al.]. Luminescent properties of Li^+ doped nanosized Y_2O_3 : Eu // Solid State Commun. 2001. Vol. 119. P. 393–396.

42. *Chen W., Kristianpoller N., Shmilevich A.* [et al.]. X-ray storage luminescence of $BaFCl : Eu^{2+}$ single crystals // J. Phys. Chem. B. 2005. Vol. 109. P. 11505–11511.

43. *Kahane S. V., Sudarsan V., Mahamuni S.* A study of charge transfer mechanism and optical properties of Au–CdS core-shell nanocrystal // J. Lumin. 2014. Vol. 147. P. 353.

44. *Xi L., Song H., Wang Y.* [et al.]. Influence of concentration effect and Au coating on photoluminescence properties of $YVO_4 : Eu^{3+}$ nanoparticle colloids // J. Phys. Chem. C. 2010. Vol. 114. P. 9975–9980.

45. *Danilkin M. I., Belousov A. P., Klimonskii S. O.* [et al.]. Formation of Eu^{2+} and Eu^{3+} centers in synthesis of CaF_2 : Eu luminophores // J. Appl. Spectrosc. 2007. Vol. 74. P. 858–865.

46. *Chaudhry A., Boutchko R., Chourou S.* [et al.]. First-principles study of luminescence in Eu^{2+}-doped inorganic scintillators // Phys. Rev. B. 2014. Vol. 89. P. 1–10.

Поступила в редакцию 21.09.2020